Exp. Theo. NANOTECHNOLOGY 10 (2026) 1219-1235 https://doi.org/10.56053/10.3.1219

Investigating the effect of additive Al_2O_3 powder on hybrid metal matrix composites in electrochemical machining with nanotechnology enhancement

Tabark M. Kadim, *Abbas F. Ibrahim*

Department of Production Engineering and Metallurgy, College of Engineering, University of Technology- Iraq, Baghdad, Iraq
*) Email: pme.24.31@grad.uotechnology.edu.iq

Received 7/4/2026, *Received in revised form* 13/6/2026, *Accepted* 28/6/2026, *Published* 15/7/2026

Metal matrix composites (MMCs) are fabricated using an advanced technique known as electrochemical fabrication (ECM). This paper investigates the feasibility of fabricating aluminum alloy 6063 reinforced with silicon carbide (SIC) and boron carbide (B4C) in metal composites in the presence of aluminum oxide (Al2O3), and examines the effects of applied voltage, electrolyte concentration, and metal rotation speed on the metal removal rate (MRR). Analysis of variance (ANOVA) revealed that the most significant factor is electrolyte concentration, followed by the applied voltage. The camshaft speed is the least influential factor, with the maximum metal removal rate reaching 77.45 mg/sec. The addition of alumina (Al_2O_3) resulted in a slight improvement in the metal removal rate, reaching 77.89 mg/sec. These results indicate that the presence of alumina particles enhances the performance of the electrochemical process. This paper presents a statistically proven optimization strategy for aerospace and automotive applications. Furthermore, the incorporation of Al_2O_3 particles can be interpreted from a nanotechnology perspective, where nanoscale reinforcement enhances electrochemical interactions, improves ion transport, and promotes more efficient material removal. This nano-enhanced approach contributes to improved machining performance and opens new opportunities for advanced manufacturing applications.

Keywords: Electrochemical machining; MRR; Taguchi technique; Al_2O_3, AMMCs. nanotechnology; nanoparticles; nano-enhanced machining; nanoscale reinforcement.

1. INTRODUCTION

Electrochemical machining (ECM) has emerged as one of the most promising non-traditional machining techniques for processing electrically conductive materials that are difficult to machine using conventional methods [1-5]. Owing to its ability to machine complex geometries with high dimensional accuracy, excellent surface integrity, ECM operates without direct contact between the tool and the workpiece, thereby eliminating mechanical stresses and thermal damage [6-10]. These distinctive characteristics make ECM particularly suitable for machining advanced materials, including aluminum metal matrix composites (AMMCs), The process is based on the principle of anodic dissolution, in which material is removed from the workpiece such that the geometry of the tool electrode is accurately reproduced on its surface [11-13]. In ECM, both the tool electrode and the workpiece are immersed in an electrically conductive electrolyte, typically an aqueous salt solution such as sodium chloride (NaCl) or sodium nitrate ($NaNO_3$) [14-17]. A constant potential difference is applied between the two electrodes, ensuring that the workpiece acts as the anode (positive electrode) [18-20]. This applied voltage initiates a direct current flow through the electrolyte, leading to controlled dissolution of the anodic material [21, 22]. At the cathode, the predominant electrochemical reaction is the evolution of hydrogen gas [23-25]. ECM systems are primarily utilized in the aerospace and aviation industries, particularly for blade profiling applications [1, 2], tool wear is negligible in ECM due to the absence of physical contact between the tool electrode and the workpiece [26-30]. This non-contact nature enables the efficient machining of complex shapes in a single operation [31-35]. In addition, ECM is capable of achieving high material removal rates (MRR) at relatively low operating voltages compared to other machining processes [36-40].

The low temperatures generated during ECM prevent thermal damage to the workpiece, thereby preserving its metallurgical properties [3, 4]. The primary objective of ECM is the controlled and precise removal of material from the workpiece [5]. Copper is an effective tool that is extensively utilized for achieving smooth finishes on workpieces [6]. Aluminum metal matrix composites (AMMCs) are increasingly utilized in aerospace and automotive industries due to their superior properties, including low wear rate and high strength-to-weight ratio [7]. In this context, the present study investigates the effects of electrolyte concentration (EC), applied voltage (V), and machining speed (S) on the material removal rate (MRR) during the ECM process [8]. Several previous studies have focused on enhancing the material removal rate and improving surface quality to produce high-precision components [41-45]. The author in [9] employed ECM to examine the influence of machining parameters such as voltage (V), electrolyte concentration (EC), and inter-electrode gap (IEG) on the material removal rate (MRR) during the machining of Al–7.5% B_4C metal matrix composites fabricated using the stir casting method [46-50]. The process parameters were optimized using the Taguchi design method, and analysis of variance (ANOVA) is applied to evaluate the statistical significance of each parameter. The results indicated that the MRR increased with higher electrolyte concentration and reduced with increased voltage and inter-electrode gap. The optimal parameter combination for maximum MRR is reported as an electrolyte concentration of 30 g/L, an applied voltage of 18 V, and an inter-electrode gap of 0.2 mm. Here is the academic rephrasing in English, with numerical values expressed scientifically rather than explicitly stated [10] utilized aluminum alloy (7075) with 5 and 10 wt.% of B_4C in two distinct amounts as reinforcement to fabricate metal matrix composites. Stir casting is employed to fabricate AMMC specimens. Utilizing ECM,A comparative investigation of the machinability of various composites is recommended. The machining speed and overcut are considered as the output response. A thermocouple is employed to continually monitor the temperature of the sodium nitrate electrolyte, which is heated by an induction heater during the machining process. The findings indicate that machining speed rises with elevated electrolyte temperature, resulting in a reduced overcut of Al7075 with a 10% mass fraction of B_4C composite. [11] concentrated on examining the influence of electrochemical machining (ECM) on the dissolving behavior of Ti-48Al-2Cr-2Nb alloy, both in the absence and presence of a magnetic field, utilizing morphological observation and other techniques. Electrochemical techniques. The electrolyte solution comprised 500 cc of $NaNO_3$ with a mass concentration of 20%. The findings indicate that employing a magnetic field during the electrochemical corrosion of titanium alloy enhances the velocity of the adsorption reaction and mitigates fluctuations in current density. The results indicate that electrochemical machining of the titanium alloy enhances corrosion uniformity through the influence of the magnetic field, facilitating the formation of an isotropic microscopic surface. Figure 1 show electrochemical machining.

The aim of this research is manufacturing the metal matrix composite (Al with4.5% SiC& 4.5%B_4C) and studying the effect of adding Al_2O_3 in electrolyte on the material removal rate (MRR), estimating the optimum parameters to estimate the material removal rate using the Taguchi method [12].

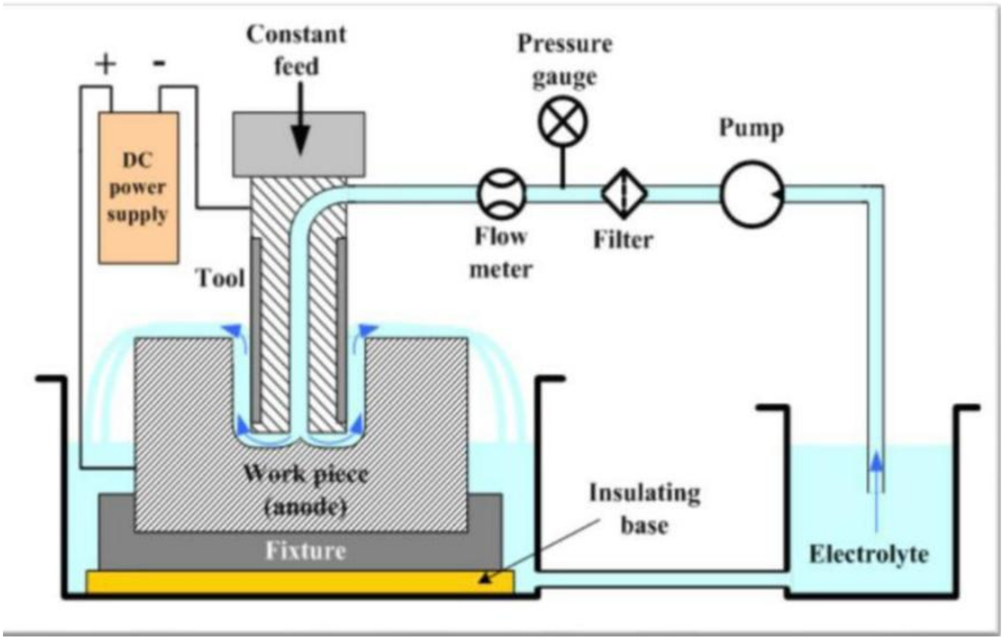

Figure 1 Diagram of electrochemical machining [12].

Recent advances in nanotechnology have enabled the use of nano-sized particles to enhance machining processes. In electrochemical machining, nanoscale additives such as Al_2O_3 improve electrolyte conductivity, mass transport, and surface interactions. These nanotechnology-driven enhancements contribute to higher machining efficiency, improved surface quality, and more stable electrochemical behavior [13-15].

2. EXPERIMENTAL WORK

2.1. Preparation of the materials

The alloy utilized to create the machined work- piece is Al6063. In this regard. Al6063 alloy is a well-known alloy widely used in industries such as automobiles, aircraft, construction, and electronics, due to its excellent properties in terms of light weight and corrosion resistance. . In this regard. Al-4.5%sic and Al-4.5%b4c workpiece materials are also used. Al-4.5% SiC and Al-4.5% B_4C workpiece materials are also used. In addition to Al6063 alloy, to produce Al-4.5% B_4C and Al-4.5 SiC, Al6063 aluminum alloy is melted in a furnace containing a crucible. The molten material is then mixed with 4.5% SiC powder to produce Al-SiC and 4.5% B_4C powder to produce Al-B_4C using a stir-casting technique at a temperature of 750°C. Continue stirring for 8 minutes after adding the powder. Then, as shown in Figure 1, a portable drill with a speed between 300-600 rpm is used to perform the stirring casting process. ahandheld drill with a speed of 300-600 RPM is used to perform the casting process by stirring. The sample dimensions were (10×10×30). The experiment is conducted using a copper tool with a diameter of 12 mm and a length of 54 mm due to its high electrical conductivity.

Figure 2 Melting process of Al6063 alloy.

2.2. The used electrolyte

Three distinct concentrations of NaCl electrolyte solution (10, 20, and 30) g/l were used in this experiment.

2.3. The used Aluminum oxide (Al_2O_3)

Aluminum oxide acts as a fine abrasive that helps remove the surface layer more quickly [13]. Al_2O_3 powder is added to an electrolyte solution consisting of sodium chloride (NaCl) at fixed concentrations and ratios. Three formulations of the electrolyte solution mixed with the powder were used:

1. A mixture of 10 wt.% NaCl + 1 wt.% Al_2O_3, consisting of 25 g of NaCl and dispersing 2.5 g of Al_2O_3 in 1L of water.
2. A second mixture containing 20 wt.% NaCl + 2 wt.% Al_2O_3, consisting of 50 g of NaCl and 5 g of Al_2O_3 in 1L of water.

3. A third mixture containing 30 wt.% NaCl + 30 wt.% Al_2O_3, consisting of 75 g of NaCl and 7.5 g of Al_2O_3 in 1L of water.

Table 1. Chemical compositions of Al+4.5%SiC+4.5B_4C

Al	Si	Fe	Cu	Mg	Zn	Ni	Pb	B
96.6	0.693	0.152	0.606	0.502	0.758	0.100	0.505	0.001

2.4. Experimental setup

The experimental investigations were performed using a Mark Super S TV1000 drilling machine, which is systematically retrofitted to function as an electrochemical machining (ECM) system. The conversion involved the integration of essential auxiliary units required to ensure stable and controlled ECM operation. A rigid workpiece fixture is employed to securely position the workpiece on the work table, thereby minimizing vibrations and ensuring dimensional accuracy during machining. The electrode is precisely aligned and fixed using a dedicated tool holder mounted above the machining zone.In addition, a dielectric fluid tank coupled with a water pump is incorporated to facilitate continuous circulation and recirculation of the electrolyte throughout the machining process. Electrical parameters were continuously monitored using a DC multimeter to ensure process stability and repeatability. The complete experimental configuration and the principal ECM components utilized in this study are schematically illustrated in Figure 3.

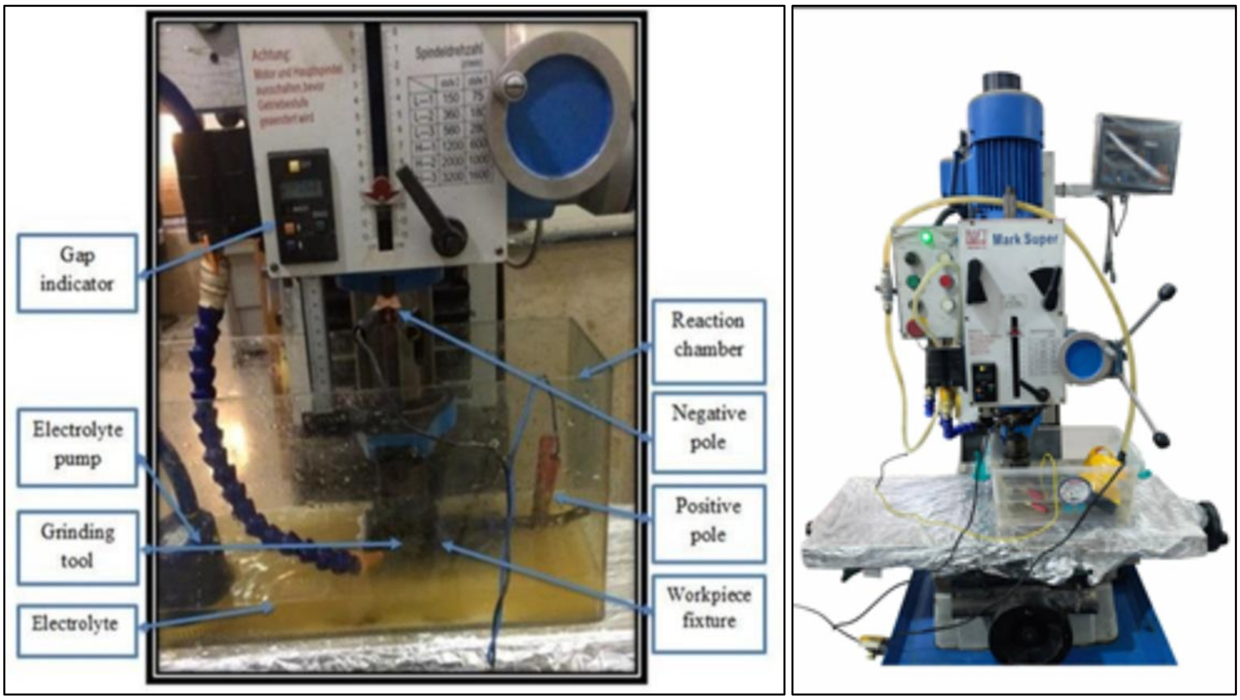

Figure 3 ECM machining.

2.5. Process parameters

A structured multi-level experimental design is implemented using Minitab 20 to plan the experimental trials efficiently. The primary input parameters selected for investigation were electrolyte concentration (g/L), applied voltage (V), and rotational speed (rpm), each examined at different levels. To evaluate the influence of machining parameters on the material removal rate (MRR), three independent process variables were considered, with each variable defined at three distinct levels [16-20]. The experimental matrix is developed based on the Taguchi L9 orthogonal array, as presented in Table 1, allowing for a systematic assessment of parameter effects with a minimized number of experimental runs. The selected parameters were analyzed to determine their individual and combined contributions to the MRR response. The corresponding machining conditions and experimental outcomes are summarized in Table 3. Each experimental trial is performed for a fixed machining time of five minutes to ensure adequate material removal and consistent surface machining across all experiments.

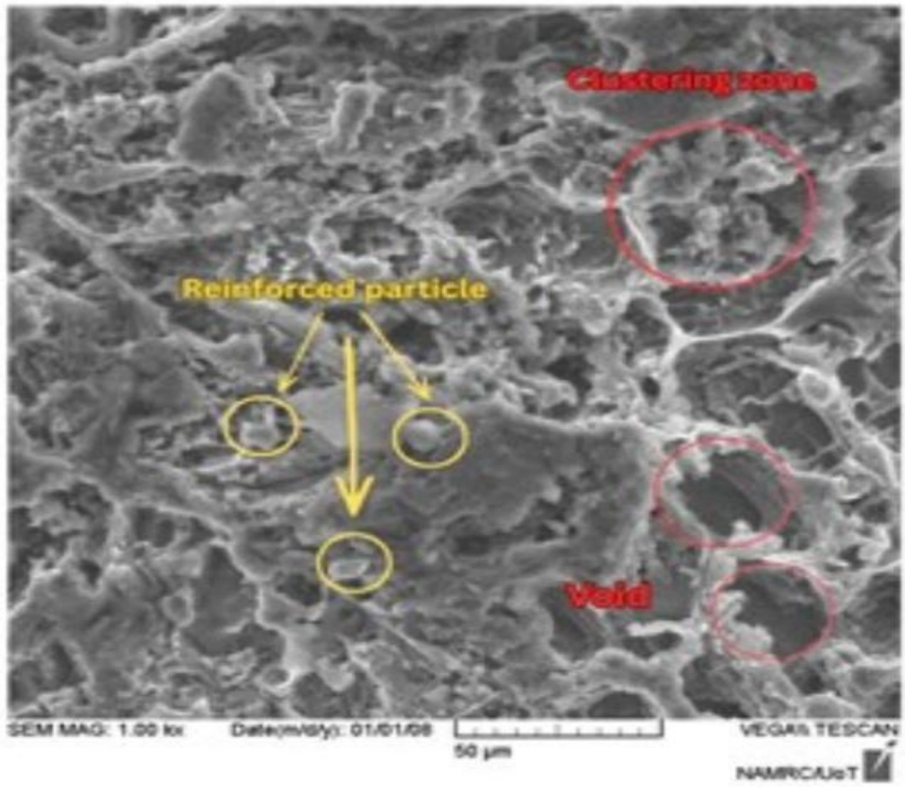

Figure 4 AL-4.5%SIC&4.5%B_4C.

2.6. Tests and inspections

The microstructure of casting samples prepared from composites made of aluminum 6063 with 4.5% silicon carbide and 4.5% boron carbide is evaluated using scanning electron microscopy (SEM). Figure 4 shows the SEM analysis, highlighting the main micro-defects affecting the mechanical properties, including crack propagation, porosity agglomeration, and reinforcement distribution. Optimizing manufacturing parameters is crucial to mitigating these defects. Figure 5 shows the base aluminum

6063 alloy with its particle distribution (silicon carbide and boron carbide). This analysis is conducted at the Nanotechnology Center of the University of Technology in Baghdad, Iraq [21-25].

Table 3 The input parameters and their levels

No	Process parameters	code	Level 1	Level 2	Level 3
1	Concentration (g/l)	A	10	20	30
2	Volt (V)	B	15	20	25
3	Speed (Rpm)	C	75	180	280

Table 4 The ECM input parameters

Run order	Concentration (g/l)	Volt (V)	Speed (Rpm)
1	10	15	75
2	10	20	180
3	10	25	280
4	20	15	180
5	20	20	280
6	20	25	75
7	30	15	280
8	30	20	75
9	30	25	180

2.7. Nanotechnology perspective in electrolyte enhancement

From a nanotechnology viewpoint, the addition of Al_2O_3 particles introduces nanoscale reinforcement into the electrolyte, which enhances ion mobility, promotes uniform current distribution, and improves the electrochemical dissolution process. These nanoparticles act as micro-agitators within the machining gap, increasing reaction efficiency and improving overall machining performance [26-30].

3. RESULTS AND DISCUSSION

3.1. Machining parameters effect on the MRR

The MRR is a crucial performance indicator in ECM, influencing the machining efficiency, productivity, and quality of the machined components [14, 15]. MRR is measured With and without the addition of Al_2O_3 to the electrolyte as depicted in Figure 4. The results show that, significantly impacts the MRR in ECM [31]. Increasing the voltage difference from (15 to 25) V led to an increase in the rate of metal removal MRR from 40.773 mg/min to 57.523 mg/min . However, when alumina Al_2O_3 is added, the MRR increased from 53.2 mg/min to 65.826 mg/min, as shown in Figure 4. The addition of aluminum oxide (Al_2O_3) particles to the electrolyte enhances the metal removal efficiency at a constant applied voltage [32]. These particles improve the hydrodynamic behavior within the inter-electrode gap by promoting electrolyte agitation and enhancing mass transport, while simultaneously reducing the accumulation of electrochemical reaction products on the workpiece surface [33]. This combined electrochemical–mechanical interaction strengthens the responsiveness of the metal removal rate to increases in the applied voltage, thereby rendering particle-assisted ECM more efficient and stable than conventional ECM processes without particulate additives [16, 17, 18]. The same figure demonstrates that, even without the addition of Al_2O_3. The electrolyte concentration plays a significant role in determining the MRR [34]. A progressive increase in electrolyte concentration from 10 g/L to 30 g/L resulted in a marked improvement in MRR, increasing from (25.006 to 72.693) mg/min, respectively. This behavior can be attributed to the strong dependence of the ion transport process within the inter-electrode gap on the electrolyte concentration [35-40]. In particular, increasing the electrolyte concentration enhances the electrical conductivity of the solution, thereby lowering the electrical resistance across the machining gap and promoting more efficient anodic dissolution [19]. As illustrated in Figure 5, the incorporation of aluminum oxide particles led to a noticeable enhancement in the material removal rate (MRR). Specifically, increasing the electrolyte concentration from 10 g/L to 30 g/L resulted in an increase in MRR from (46.616 to 71.117) mg/min. These findings suggest that the presence of aluminum oxide positively influences electrolyte flow behavior and enhances ion mobility within the machining gap, thereby improving the overall electrochemical machining performance [41, 42]. In essence, the MRR is significantly impacted by Speed of rotation of the tool utilized in the ECM process we observe that the metal removal rate before adding aluminum oxide (Al_2O_3) is 45.116 mg/min, while the removal rate increased to 51.81 mg/min. This indicates that tool rotation facilitates higher ionic mobility and continuous renewal of the electrolyte within the machining gap [43-45]. The observed improvement can be ascribed to enhanced electrolyte flow patterns and the more efficient evacuation of hydrogen gas bubbles and reaction by-products from the inter-electrode region, collectively leading to a more effective anodic dissolution process [20, 21]. However, after adding Al_2O_3, the removal rate increased to 59.88 and to 60.036 at%.

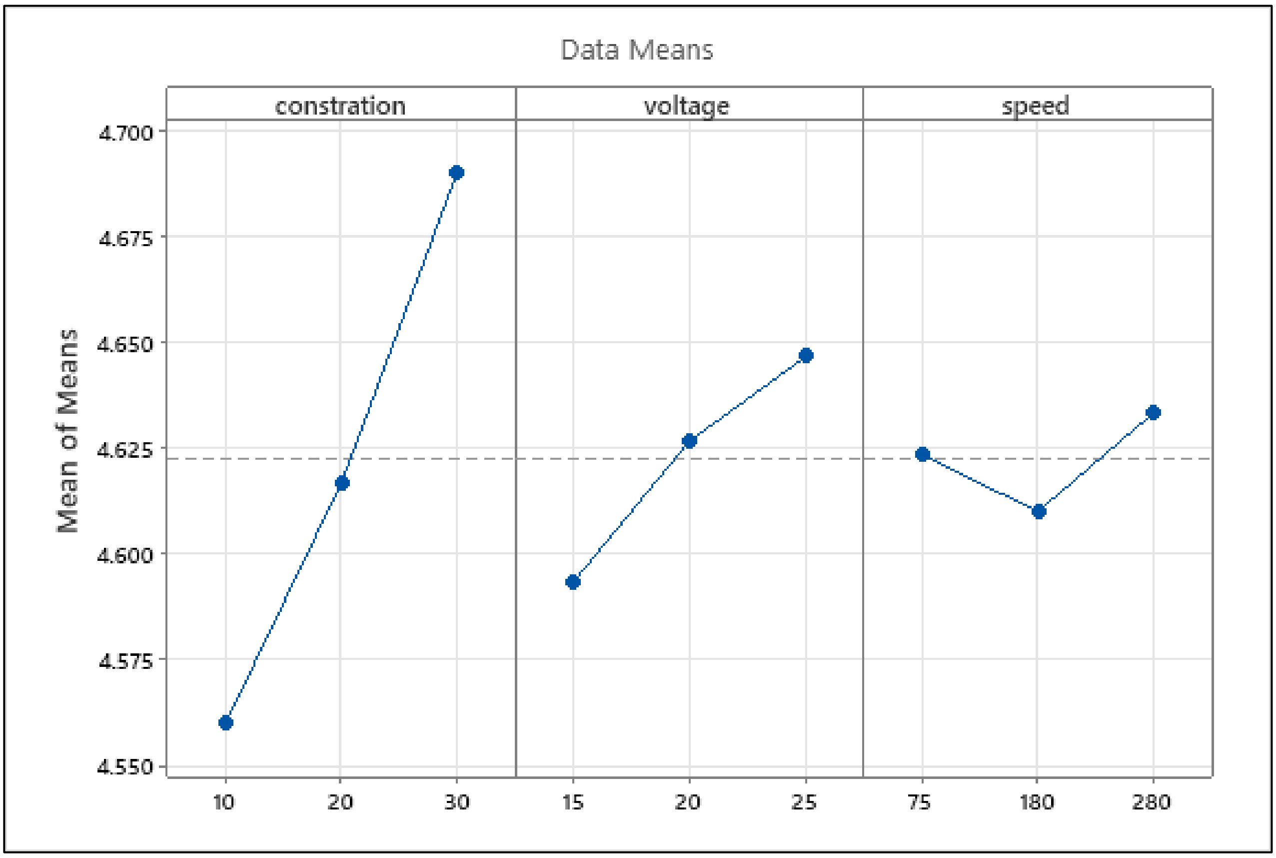

Figure 5 Main effects plot for MRR without adding Al_2O_3 in ECM.

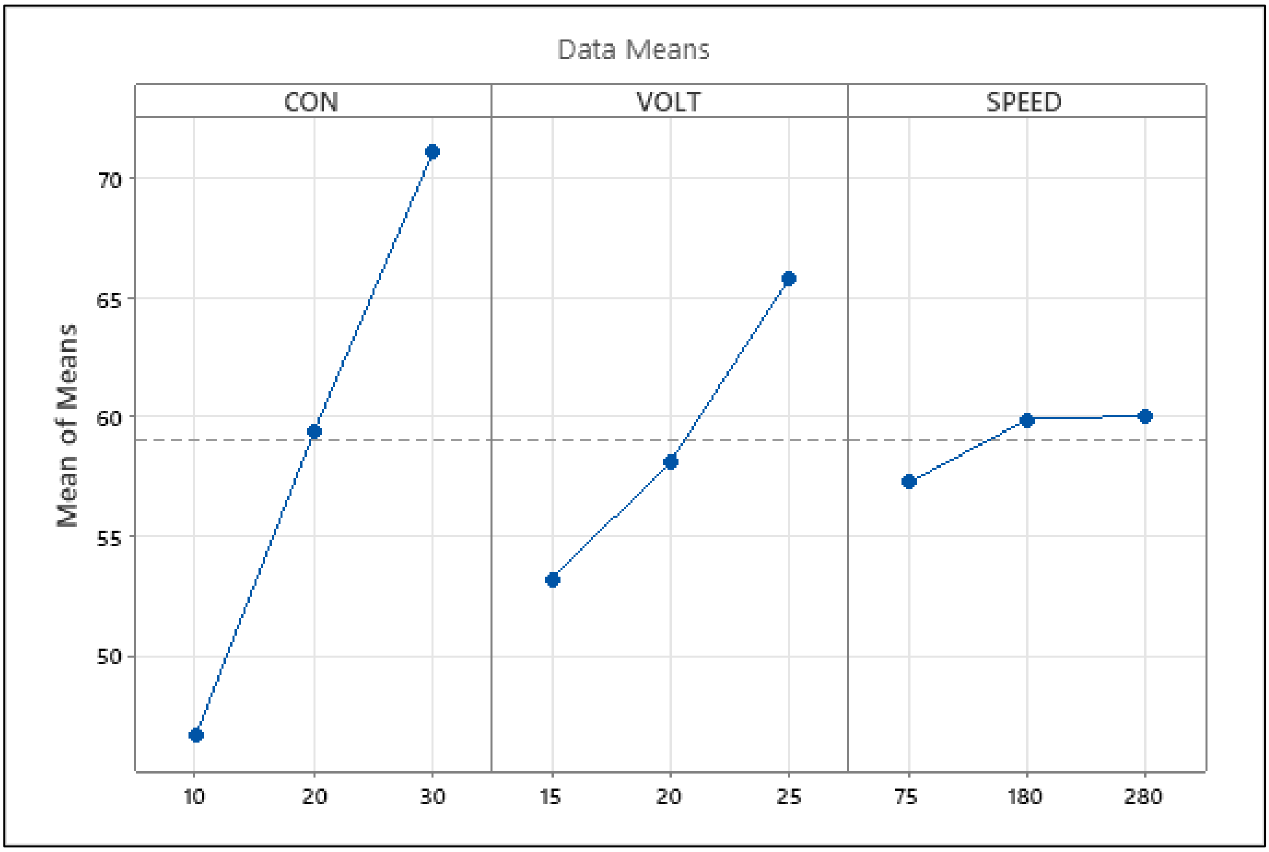

Figure 6 Main effects plot for MRR withadding Al_2O_3 in ECM.

The Table 3 demonstrates that higher voltage, electrolyte concentration, and rotaition speed improved MRR in ECM for both with and without adding aluminum oxide Al_2O_3. as show from the table, Overall, the incorporation of aluminum oxide (Al_2O_3) particles resulted in a consistent enhancement of the metal removal rate (MRR), indicating a notable improvement in machining efficiency [45-50]. This improvement can be attributed to the favorable influence of Al_2O_3 on electrolyte behavior, including enhanced ion transport and more effective removal of reaction products from the machining zone. The experimental results demonstrate that, across all operating conditions, higher MRR values were achieved when aluminum oxide is added to the electrolyte [51-53]. Under the optimal machining parameters (Experiment 9: 25 V, 30 g/L, 180 rpm), the maximum MRR of 77.89 mg/L is obtained, confirming the positive role of Al_2O_3 in promoting more efficient anodic dissolution during the ECM process [54, 55]. Figure 6 illustrates the variation in metal removal rate (MRR) with and without the addition of aluminum oxide to the electrolyte across experiments (1–9). The results reveal that the MRR values obtained with aluminum oxide addition are consistently higher than those recorded without its inclusion, indicating a clear enhancement in material removal performance. This improvement can be attributed to the role of aluminum oxide particles in facilitating the removal of electrochemical reaction by-products, such as hydrogen gas bubbles and metal hydroxides, thereby improving the stability and efficiency of the machining process.

Table 5 The ECM parameters' results

Run	Concentration	Voltage	Speed	MRR with out adding Al_2O_3	MRR with adding Al_2O_3
1	10	15	75	20.12	38.12
2	10	20	180	24.1	46.5
3	10	25	280	30.8	55.23
4	20	15	180	33.8	55.25
5	20	20	280	56.23	58.65
6	20	25	75	64.32	64.36
7	30	15	280	68.4	66.23
8	30	20	75	72.23	69.23
9	30	25	180	77.45	77.89

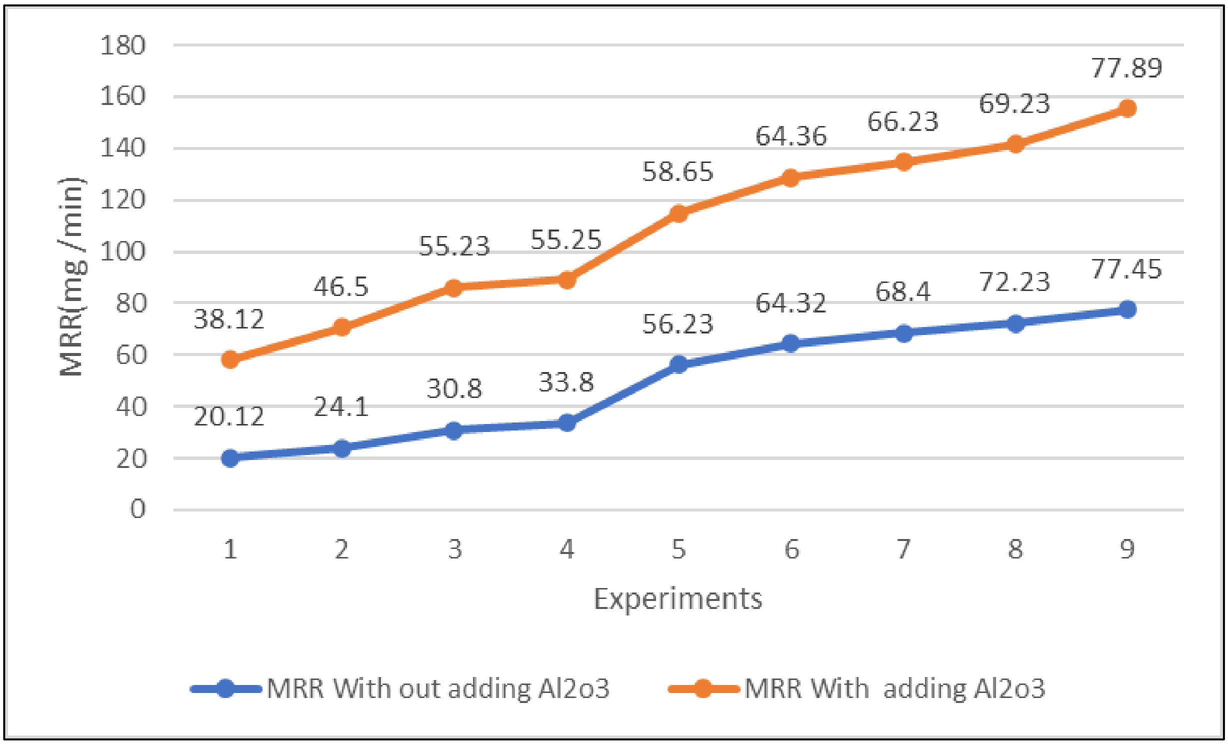

Figure 7 MRR results with and without magnetic field.

3.2. Analysis of variance (ANOVA)

The data on the analysis of variance (ANOVA) for the MRR of ECM with and without adding Al_2O_3 are shown in Tables 6 and 7. The ANOVA results reveal a distinct difference in the material removal rate (MRR) behavior between the conventional electrochemical machining (ECM) process and adding the Al_2O_3 to electrolyte. In the conventional ECM configuration, electrolyte concentration exhibited a statistically significant influence on MRR, whereas voltage did not show a significant effect at a 95% confidence level [56]. This indicates that the process behavior is predominantly governed by ionic transport and mass transfer mechanisms within the inter-electrode gap. Increasing electrolyte concentration enhanced ionic conductivity and reduced anodic polarization, thereby promoting anodic dissolution, while further increases in voltage resulted in a limited contribution due to the onset of current density saturation [57]. Conversely, in the Al_2O_3-assisted ECM system, both electrolyte concentration and voltage demonstrated statistically significant effects on MRR, with electrolyte concentration remaining the dominant parameter. The presence of Al_2O_3 particles enhances flow turbulence within the inter-electrode gap, facilitates the removal of reaction products, and reduces the thickness of the passive layer on the anodic surface. Consequently, the applied voltage becomes more effective in increasing the current density and intensifying the electrochemical reaction, leading to a substantial improvement in MRR [58]. These findings confirm that the incorporation of Al_2O_3 particles not only enhances the material removal rate but also alters the governing mechanism of the ECM process from a mass-transport-limited regime to a more voltage-responsive system, while preserving the dominant role of electrolyte concentration. This transition highlights the synergistic electrochemical–mechanical effect induced by particle-assisted ECM [59].

Table 6 The ANOVA table for the measured MRR without adding Al_2O_3

Source	DF	Adj SS	Adj MS	F-Value	P-Value
Concentration	2	3424.5	1712.27	39.62	0.002
Voltage	2	426.7	213.33	4.94	0.083
Error	4	172.9	43.22		
Total	8	4024.1			

Table 7 The ANOVA table for the measured MRR with adding Al_2O_3

Source	DF	Adj SS	Adj MS	F-Value	P-Value
CON	2	900.99	450.494	94.32	0
VOLT	2	242.99	121.497	25.44	0.005
Error	4	19.1	4.776		
Total	8	1163.09			

3.3. Predicting the optimum value of MRR response

Based on the methodology described above, an optimality search model is developed to identify the most suitable combinations of process parameters for enhancing the metal removal rate (MRR) of the machined workpieces. Regression analysis is applied to examine the relationship between the input process variables and the resulting machining performance. By utilizing Equations (1) and (2), the combined influence of the machining parameters is evaluated, enabling the determination of the optimal parameter settings that achieve the desired response. to correlate the influence of the selected process variables on the metal removal rate (MRR) is investigated both in the absence and presence of Al_2O_3 particles in the electrolyte. A mathematical relationship describing the MRR without the addition of Al_2O_3 is established based on the considered process variables, as presented below [60, 61].

$$MRR(mg/min) = 49.72 - 24.71\ X1\_10 + 1.73\ X1\_20 + 22.98\ X1\_30 - 8.94\ X2\_15 + 1.14\ X2\_20 + 7.81\ X2\_25 \quad (1)$$

A mathematical relationship describing the metal removal rate (MRR) in the presence of Al_2O_3 particles is developed based on the selected process variables, as expressed below

MRR(mg/min) = 59.051 - 12.43 X1_10 + 0.37 X1_20 + 12.07 X1_30 - 5.85 X2_15 - 0.92 X2_20+ 6.78X2_25 (2)

where: X1 – concentration (g/l), X2 – voltage (V),

Table 8 Response table of means for MRR without adding Al_2O_3.

Level	Concentration	Voltage	Speed
1	27.83	31.12	33.14
2	33.91	33.27	32
3	37.22	34.57	33.82
Delta	9.39	3.46	1.82
Rank	1	2	3

Table 9 Response table of means for MRR with adding Al_2O_3.

Level	Concentration	Voltage	Speed
1	33.27	34.3	34.87
2	35.46	35.17	35.34
3	37.02	36.28	35.54
Delta	3.75	1.98	0.68
Rank	1	2	3

The model summary figures provide a clear indication of the adequacy of the developed regression models in representing the experimental data. The coefficient of determination R-Square is employed as a primary statistical indicator to evaluate the goodness of fit of the proposed models. In addition, the adjusted coefficient of determination R -sq(adj), which accounts for the number of model terms, is used to ensure a more reliable assessment of model performance. Generally, higher values of R-Square R-sq(adj) reflect a stronger agreement between the predicted and experimental results. Tables 10 and 11 present the R-Square and R-sq(adj), and predicted R-Square R-sq(pred) values for the mathematical models developed to describe the metal removal rate (MRR) with the incorporation of Al_2O_3 particles into the electrolyte. The obtained results demonstrate a noticeable enhancement in model performance when Al_2O_3 is added, indicating an improved capability of the machining model to accurately explain and predict variations in MRR. Notably, the R-sq(pred) value increased from 89.91% to 97.43%, confirming that the presence of aluminum oxide particles contributed to a more stable and reliable material removal process [62, 63].

Table 10 Model summary of MRR without adding Al_2O_3 for the machining variables.

S	R-sq	R-sq(sdj)	R-sq(pred)
5.66012	95.22%	93.63%	89.91%

Table 11 Model summary of MRR with adding Al_2O_3 for the machining variables.

S	R-sq	R-sq(sdj)	R-sq(pred)
1.5254	99.00%	98.40%	97.43%

Table 12 Prediction accuracy of MRR with adding Al_2O_3

Concentration	Volt	Speed	MRR (mg/min) EXP	MRR (mg/min) Pred	Error (%)
10	15	75	38.12	39.06648692	2.48291
10	20	180	46.5	46.82403516	0.69685
10	25	280	55.23	54.51281126	1.298549
20	15	180	55.25	52.76070182	4.505517
20	20	280	58.65	60.44947793	3.06817
20	25	75	64.36	63.94315358	0.647679
30	15	280	66.23	66.38614459	0.23576
30	20	75	69.23	69.87982025	0.93864
30	25	18	77.89	77.63736849	0.324344

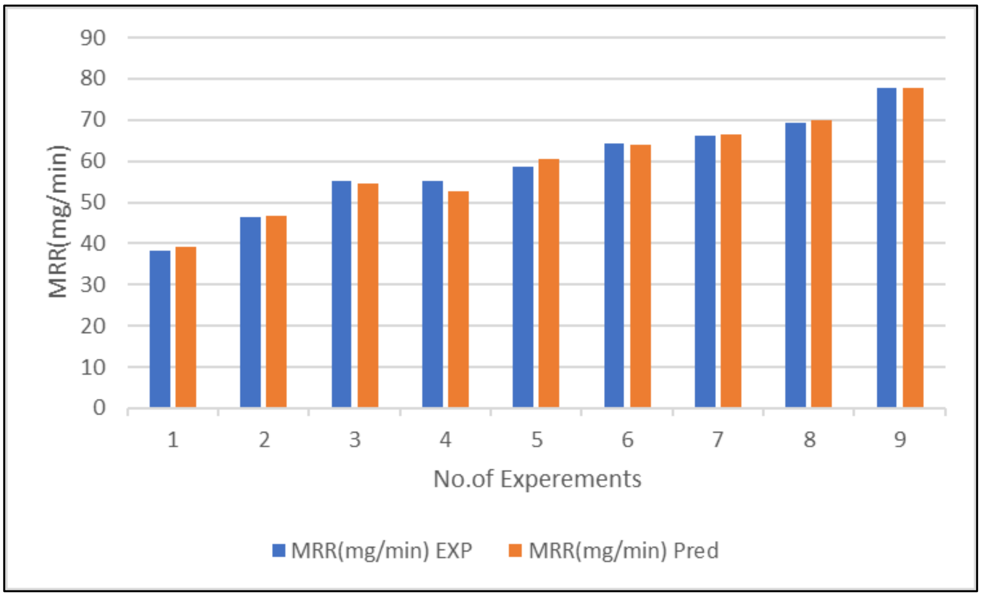

Figure 8 Experimental and predicted value of MRR with adding Al_2O_3.

In light of the observed enhancement in performance resulting from the incorporation of Al_2O_3 into the electrolyte, the reliability of Equation (2) is systematically assessed. Accordingly, the predicted values of the material removal rate (MRR) in the presence of aluminum oxide (Al_2O_3) were determined. The outcomes of this evaluation confirm that the developed predictive model demonstrates satisfactory accuracy. Table 12 presents a comparative analysis between the experimentally measured and model-predicted MRR values. The results reveal that the relative deviations remain minimal, indicating a strong correlation between experimental observations and predicted outcomes. Furthermore, Figure 7 illustrates this close agreement for the MRR values obtained with the addition of Al_2O_3, thereby validating the robustness and predictive capability of the proposed mode.

3.4. Effect of nanotechnology on ECM performance

The presence of Al_2O_3 particles significantly enhances the material removal rate due to nanotechnology-driven mechanisms such as improved ion transport, enhanced turbulence, and better removal of reaction by-products. These nanoscale effects lead to more efficient anodic dissolution and improved machining stability [64]. Table 13 presents the improvement in electrochemical machining performance due to nanotechnology-enhanced electrolyte behavior.

Table 13 Comparison between conventional ECM and nanotechnology-enhanced ECM using Al_2O_3 particles.

Parameter	Conventional ECM	Nano-Enhanced ECM
Ion Transport	Moderate	Enhanced
Surface Interaction	Standard	Improved
Reaction Stability	Moderate	High
MRR Performance	Good	Excellent
Efficiency	Moderate	Enhanced

Figure 9 presents the variation of MRR with and without the addition of Al_2O_3, demonstrating a consistent improvement in machining performance due to nanoparticle-assisted electrochemical machining.

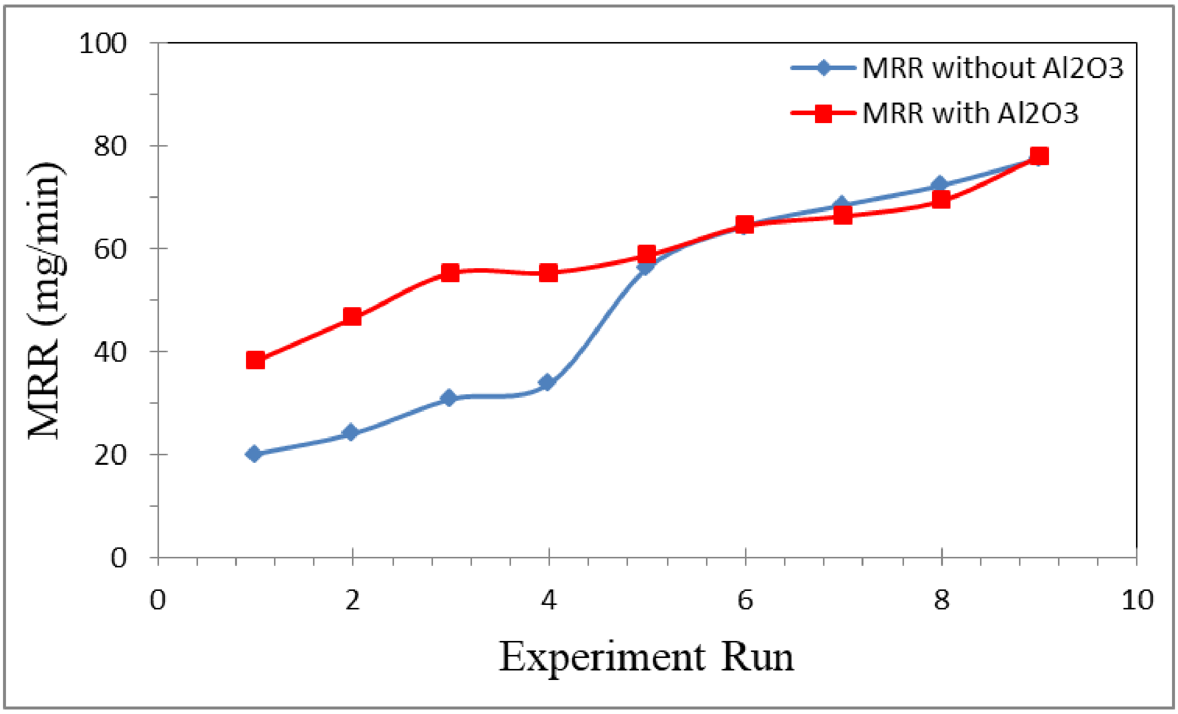

Figure 9 Effect of Al_2O_3 addition on material removal rate (MRR) across experimental runs.

4. CONCLUSIONS

This study investigates the influence of operating parameters on the material removal rate (MRR) in electrochemical machining, both in the absence and presence of aluminum oxide (Al_2O_3) particles in the electrolyte. A comparative evaluation of the electrochemical process performance was conducted across all experimental conditions. The findings demonstrate that the incorporation of Al_2O_3 into the electrolyte markedly alters the electrochemical reactions occurring at the interface between the electrically charged workpiece and the electrolyte medium. The presence of Al_2O_3 enhances the transport dynamics of charged species by intensifying the induced current, thereby accelerating the migration of metal cations from the workpiece and the flow of electrons toward the tool. As a result, metal ions originating from the aluminum-based composite material reinforced with Al_2O_3 (4.5 wt.%), SiC (4.5 wt.%), and B_4C are transported more rapidly within the inter-electrode gap, leading to improved electrochemical dissolution behavior. This effect can be attributed to the role of aluminum oxide particles in modifying the mobility and concentration of active ions, which ultimately enhances the efficiency of the electrochemical removal process. These outcomes underscore the considerable potential of Al_2O_3-assisted electrolytes in regulating electrochemical reactions and improving ion removal efficiency in a wide range of industrial and scientific applications. The scanning electron microscope image shows the surface morphology of the composite material with a metallic matrix reinforced with silicon carbide and boron carbide particles. The images above reveal particle aggregation, where the B_4C and SiC particles tend to cluster in specific areas rather than being uniformly distributed within the metallic matrix. This irregular distribution can be attributed to differences in density, wettability, and manufacturing conditions. Furthermore, the surface structure exhibits irregularities, including pits and voids, indicating particle segregation and weak interfacial bonding between the matrix and reinforcing materials. The contrast differences in the image also reflect a clear distinction between the metallic and ceramic phases, generally indicating heterogeneity in the microstructure and localized defects within the hybrid composite material. The incorporation of Al_2O_3 particles from a nanotechnology perspective significantly enhances electrochemical machining performance by improving ion transport, reaction stability, and material removal efficiency. This study confirms that nano-enhanced electrolytes provide a promising approach for advanced manufacturing, enabling higher precision, efficiency, and process stability in hybrid metal matrix composites.

References

[1] I. M. Mohammed, M. Rasheed, AIP Conference Proceedings, 3321 (2025) 020026. https://doi.org/10.1063/5.0289719.
[2] A. Khaleefah, M. RASHEED, Experimental and Theoretical NANOTECHNOLOGY, 10 (2026) 289. https://doi.org/10.56053/10.s.289.
[3] I. A. Ali, M. RASHEED, Experimental and Theoretical NANOTECHNOLOGY, 10 (2026) 277. https://doi.org/10.56053/10.s.277.
[4] I. A. Ali, M. RASHEED, Experimental and Theoretical NANOTECHNOLOGY, 10 (2026) 239. https://doi.org/10.56053/10.s.239.
[5] M. Rasheed, et al., Journal of Advanced Biotechnology and Experimental Therapeutics, 6 (2023) 495. https://doi.org/10.5455/jabet.2023.d144.
[6] E. Kadri, et al., Journal of Alloys and Compounds, 705 (2017) 708. https://doi.org/10.1016/j.jallcom.2017.02.117.
[7] M. Rasheed, R. Barillé, Journal of Alloys and Compounds, 728 (2017) 1186. https://doi.org/10.1016/j.jallcom.2017.09.084.
[8] R. S. Mahmood, et al., Journal of the Mechanical Behavior of Materials, 34 (2025) 1. https://doi.org/10.1515/jmbm-2025-0040.
[9] M. Rasheed, A. Khaleefah, Materials Chemistry and Physics, 355 (2026) 132112. https://doi.org/10.1016/j.matchemphys.2026.132112.
[10] F. Boudou, et al., Notulae Scientia Biologicae, 17 (2025) 12593. https://doi.org/10.55779/nsb17312593.
[11] A. Ruszaj, *Mechanik*, 90 (2017) 1102. https://doi.org/10.17814/mechanik.2017.12.188.
[12] K. Salman, A. F. Ibrahim, *AIP Conference Proceedings* (2025) 040090. https://doi.org/10.1063/5.0258059.
[13] F. Ibrahim, *Al-Khwarizmi Engineering Journal*, 12 (2017) 72. https://doi.org/10.22153/kej.2016.06.001.
[14] Z. Pandilov, *IOP Conference Series: Materials Science and Engineering*, 329 (2018) 012014. https://doi.org/10.1088/1757-899X/329/1/012014.
[15] A. F. Ibrahim, *Journal of Physics: Conference Series*, 1973 (2021) 012154. https://doi.org/10.1088/1742-6596/1973/1/012154.
[16] B. Abdulwahhab, A. F. Ibrahim, *AIP Conference Proceedings* (2025) 030004. https://doi.org/10.1063/5.0265942.
[17] Fadhil, *IIUM Engineering Journal*, 23 (2022) 349. https://doi.org/10.31436/iiumej.v23i1.2114.
[18] F. Ibrahim, S. M. Mousa, D. A. K. Noori, *Periodicals of Engineering and Natural Sciences*, 10 (2022) 48. https://doi.org/10.21533/pen.v10i3.3006.
[19] G. E. Alkinani, A. R. J. Katae, M. RASHEED, Experimental and Theoretical NANOTECHNOLOGY, 10 (2026) 1027. https://doi.org/10.56053/10.S.1027.
[20] Z. S. Ahmed, M. RASHEED, H. S. Ahmed, Experimental and Theoretical NANOTECHNOLOGY, 10 (2026) 329. https://doi.org/10.56053/10.s.329.

[21] Z. S. Ahmed, M. RASHEED, H. S. Ahmed, Experimental and Theoretical NANOTECHNOLOGY, 10 (2026) 343. https://doi.org/10.56053/10.s.343.
[22] E. Arif, R. Jamal, M. RASHEED, Experimental and Theoretical NANOTECHNOLOGY, 10 (2026) 453. https://doi.org/10.56053/10.2.453.
[23] A. J. Hussein, M. N. Al-Darraji, M. Rasheed, IOP Conference Series: Earth and Environmental Science, 1262 (2023) 022007. https://doi.org/10.1088/1755-1315/1262/2/022007.
[24] A. Abdulrahman, M. Rasheed, S. Shihab, Journal of Physics: Conference Series, 1879 (2021) 022118. https://doi.org/10.1088/1742-6596/1879/2/022118.
[25] T. Rashid, M. M. Mokji, M. Rasheed, Journal of the Mechanical Behavior of Materials, 34 (2025) 1. https://doi.org/10.1515/jmbm-2025-0074.
[26] H. K. Aity, E. Dhahri, M. Rasheed, Ceramics International, 50 (2024) 54666. https://doi.org/10.1016/j.ceramint.2024.10.324.
[27] J. Liao, X. M. Zhang, Z. J. Luo, *Journal of Applied Electrochemistry*, 53 (2023) 49. https://doi.org/10.1007/s10800-022-01756-0.
[28] T. Rashid, M. M. Mokji, M. Rasheed, Journal of Optics, 53 (2024) 1. https://doi.org/10.1007/s12596-024-02080-w.
[29] K. K. Khudair, F. Boudou, A. Mohammed, A. Sehmi, A. Belakredar, M. S. Ibrahim, Experimental and Theoretical NANOTECHNOLOGY, 10 (2026) 869. https://doi.org/10.56053/10.S.869.
[30] A. Keziz, M. Rasheed, M. Heraiz, F. Sahnoune, A. Latif, Ceramics International, 49 (2023) 37423. https://doi.org/10.1016/j.ceramint.2023.09.068.
[31] W. Saidi, N. Hfaidh, M. Rasheed, M. Girtan, A. Megriche, M. El Maaoui, RSC Advances, 6 (2016) 68819. https://doi.org/10.1039/c6ra15060h.
[32] M. S. Ibrahim, T. T. Issa, B. Yaqoob, E. N. Fayyadh, A. Rashid, R. S. Mahmood, Experimental and Theoretical NANOTECHNOLOGY, 10 (2026) 887. https://doi.org/10.56053/10.S.887.
[33] M. Rasheed, I. Alshalal, A. A. Rashed, M. A. Sarhan, A. S. Jaber, Indonesian Journal of Electrical Engineering and Computer Science, 33 (2024) 653. https://doi.org/10.11591/ijeecs.v33.i1.pp653-660.
[34] D. Kherifi, A. Keziz, M. Rasheed, A. Oueslati, Ceramics International, 50 (2024) 1. https://doi.org/10.1016/j.ceramint.2024.05.317.
[35] H. M. I. Al-Zuhairi, I. Alshalal, H. H. Abbood, M. Al Nuaimi, Experimental and Theoretical NANOTECHNOLOGY, 10 (2026) 855. https://doi.org/10.56053/10.S.855.
[36] H. M. I. Al-Zuhairi, I. Alshalal, H. H. Abbood, M. Al Nuaimi, Experimental and Theoretical NANOTECHNOLOGY, 10 (2026) 1093. https://doi.org/10.56053/10.S.1093.
[37] A. J. Hussein, M. N. Al-Darraji, M. Rasheed, M. A. Sarhan, IOP Conference Series: Earth and Environmental Science, 1262 (2023) 022005. https://doi.org/10.1088/1755-1315/1262/2/022005.
[38] M. Rasheed, O. Y. Mohammed, S. Shihab, A. Al-Adili, Journal of Physics: Conference Series, 1795 (2021) 012042. https://doi.org/10.1088/1742-6596/1795/1/012042
[39] Raghdi, M. Heraiz, M. Rasheed, A. Keziz, Journal of the Indian Chemical Society, 101 (2024) 101413. https://doi.org/10.1016/j.jics.2024.101413.
[40] A. Zubaidi, L. M. Asaad, I. Alshalal, M. Rasheed, Journal of the Mechanical Behavior of Materials, 32 (2023) 1. https://doi.org/10.1515/jmbm-2022-0302.
[41] E. Kadri, M. Krichen, R. Mohammed, A. Zouari, K. Khirouni, Optical and Quantum Electronics, 48 (2016) 1. https://doi.org/10.1007/s11082-016-0812-7.
[42] T. Saidani, M. Rasheed, I. Alshalal, A. A. Rashed, M. A. Sarhan, R. Barillé, Research on Engineering Structures and Materials, 9 (2023) 1. https://doi.org/10.17515/resm2023.21ma0922rs.
[43] R. J. Katae, H. H. Hussein, A. S. Jaber, M. A. Sarhan, M. RASHEED, Experimental and Theoretical NANOTECHNOLOGY, 10 (2026) 725. https://doi.org/10.56053/10.2.725.

[44] R. J. Katae, H. H. Hussein, A. S. Jaber, M. A. Sarhan, M. RASHEED, Experimental and Theoretical NANOTECHNOLOGY, 10 (2026) 795. https://doi.org/10.56053/10.2.795.
[45] A. Jaber, M. Ismael, T. Rashid, M. A. Sarhan, M. Rasheed, I. M. Sala, Eureka: Physics and Engineering, 4 (2023) 29. https://doi.org/10.21303/2461-4262.2023.002770.
[46] T. Saidani, M. Zaabat, M. S. Aida, R. Barillé, M. Rasheed, Y. Almohamed, Journal of Materials Science: Materials in Electronics, 28 (2017) 9252. https://doi.org/10.1007/s10854-017-6660-9.
[47] T. Saidani, S. Mokhtari, M. Rasheed, H. Lahmar, M. Trari, Journal of the Indian Chemical Society, 103 (2026) 102499. https://doi.org/10.1016/j.jics.2026.102499.
[48] J. Jeykrishnan, B. V. Ramnath, C. Elanchezhian, S. Akilesh, *Materials Today: Proceedings*, 4 (2017) 7884. https://doi.org/10.1016/j.matpr.2017.07.124.
[49] J. P. Chen, L. Gu, G. J. He, *International Journal of Minerals, Metallurgy and Materials*, 27 (2020) 1451. https://doi.org/10.1007/s40436-020-00313-2.
[50] F. Boudou, A. Guendouzi, A. Belakredar, M. RASHEED, Notulae Scientia Biologicae, 16 (2024) 13837. https://doi.org/10.55779/nsb16211837.
[51] F. Boudou, A. Belakredar, A. Berkane, M. RASHEED, Notulae Scientia Biologicae, 17 (2025) 12183. https://doi.org/10.55779/nsb17212183.
[52] M. Enneffati, B. Louati, K. Guidara, M. Rasheed, R. Barillé, Journal of Materials Science: Materials in Electronics, 29 (2018) 171. https://doi.org/10.1007/s10854-017-7901-7.
[53] M. Enneffati, M. Rasheed, B. Louati, K. Guidara, R. Barillé, Optical and Quantum Electronics, 51 (2019) 1. https://doi.org/10.1007/s11082-019-2015-5.
[54] F. Dkhilalli, S. Megdiche, K. Guidara, M. Rasheed, R. Barillé, M. Megdiche, Ionics, 24 (2018) 169. https://doi.org/10.1007/s11581-017-2193-8.
[55] F. Boudou, A. E. Sabar, M. I. Majeed, A. M. Ibraham, R. Jamal, A. Rashid, A. Belakredar, M. Bendahmane-Salmi, M. RASHEED, R. RASHEED, T. Saidani, H. D. Al-Bahadli, Experimental and Theoretical NANOTECHNOLOGY, 10 (2026) 821. https://doi.org/10.56053/10.S.821.
[56] A. S. Channi, H. S. Bains, J. S. Grewal, V. S. Chidambranathan, R. Kumar, *Journal of Electrochemical Science and Engineering* (2022). https://doi.org/10.5599/jese.1391.
[57] M. Rasheed, S. Shihab, O. Alabdali, A. Rashid, T. Rashid, Journal of Physics: Conference Series, 1999 (2021) 012077. https://doi.org/10.1088/1742-6596/1999/1/012077.
[58] S. S. Batros, M. Rasheed, H. K. Aity, A. A. Hatef, T. Saidani, Materials Chemistry and Physics, 355 (2026) 132243. https://doi.org/10.1016/j.matchemphys.2026.132243.
[59] M. Rasheed, M. N. Mohammedali, F. A. Sadiq, M. A. Sarhan, T. Saidani, Journal of Optics, 54 (2024) 1. https://doi.org/10.1007/s12596-024-01928-5.
[60] H. K. Aity, M. Rasheed, E. Dhahri, A. A. Hateef, T. Saidani, Journal of Materials Science, 61 (2026) 6226. https://doi.org/10.1007/s10853-026-12241-w.
[61] A. Aukštuolis, et al., Proceedings of the Romanian Academy Series A: Mathematics, Physics, Technical Sciences, Information Science, 18 (2017) 34. https://hal.archives-ouvertes.fr/hal-02443179.
[62] S. M. Mousa, S. O. Alyousifi, D. A. K. Noori, A. F. Ibrahim, *Tehnički Glasnik*, 20 (2026) 126. https://doi.org/10.31803/tg-20240404220017.
[63] Zhang, P. Zheng, R. Liang, K. Yun, X. Jiang, Z. Yan, *International Journal of Electrochemical Science*, 15 (2020) 1148. https://doi.org/10.20964/2020.02.10.
[64] A. A. Hateef, E. Dhahri, M. Rasheed, H. Kadhim, Z. Abbas, N. Hassan, *Physics and Chemistry of Solid State*, 25 (2024) 801. https://doi.org/10.15330/pcss.25.4.801-810.

© 2026 The Authors. Published by LPCMA (https://etnano.com). This article is an open access article distributed under the terms and conditions of the Creative Commons Attribution license (http://creativecommons.org/licenses/by/4.0/).